

QUANTIFYING TRAFFIC CONGESTION-INDUCED CHANGE OF NEAR-ROAD AIR POLLUTANT CONCENTRATION



June 2019



Center for Advancing Research in
Transportation Emissions, Energy, and Health
A USDOT University Transportation Center



Disclaimer

The contents of this report reflect the views of the authors, who are responsible for the facts and the accuracy of the information presented herein. This document is disseminated in the interest of information exchange. The report is funded, partially or entirely, by a grant from the U.S. Department of Transportation's University Transportation Centers Program. However, the U.S. Government assumes no liability for the contents or use thereof.

TECHNICAL REPORT DOCUMENTATION PAGE

1. Report No.	2. Government Accession No.	3. Recipient's Catalog No.	
4. Title and Subtitle Quantifying Traffic Congestion-Induced Change of Near-Road Air Pollutant Concentration		5. Report Date June 2019	
		6. Performing Organization Code	
7. Author(s) Ji Luo, Ayla Moretti, Guoyuan Wu		8. Performing Organization Report No. UCR-01-15	
9. Performing Organization Name and Address: CARTEEH UTC University of California, Riverside		10. Work Unit No.	
		11. Contract or Grant No. 69A3551747128	
12. Sponsoring Agency Name and Address Office of the Secretary of Transportation (OST) U.S. Department of Transportation (USDOT)		13. Type of Report and Period Final April 2018–April 2019	
		14. Sponsoring Agency Code	
15. Supplementary Notes This project was funded by the Center for Advancing Research in Transportation Emissions, Energy, and Health University Transportation Center, a grant from the U.S. Department of Transportation Office of the Assistant Secretary for Research and Technology, University Transportation Centers Program.			
16. Abstract The objective of this study was to examine the relationship between air quality and traffic and weather parameters. With air quality measurements spanning over 11 months, we attempted to gain better understanding of the near-freeway air pollutant concentration, traffic speed, traffic flow, and weather parameters. We applied both multiple linear regression (MLR) and multivariate adaptive regression splines (MARS) models to examine the relationship among the weather conditions, traffic states, and near-freeway air pollutant concentrations. Both MLR and MARS showed that all weather parameters (e.g., relative humidity, temperature, wind) were significant variables. For the State Route 60 air monitoring station (AMS), MLR gave the adjusted R^2 as 0.077 and 0.264 for $PM_{2.5}$ and NO_2 , respectively, and MARS gave the R^2 as 0.19 and 0.53, respectively. For the Interstate 710 AMS, MLR gave the adjusted R^2 as 0.035 and 0.324 for $PM_{2.5}$ and NO_2 , respectively, and MARS gave the R^2 as 0.11 and 0.62, respectively. Generally, NO_2 concentration can be better explained by the selected variables than can $PM_{2.5}$. The test of traffic speed segmentation indicates that the traffic speed has a considerable influence on near-road pollutant concentrations. When applying MLR and MARS models for winter months, the prediction performance for $PM_{2.5}$ improves significantly at both AMSs, but the improvement effect is moderate for NO_2 . We recommend that controlling seasonal weather variables can significantly improve $PM_{2.5}$ prediction performance.			
17. Key Words Traffic, Congestion, Meteorology, Air Pollution		18. Distribution Statement No restrictions. This document is available to the public through the CARTEEH UTC website. http://carteeh.org	
19. Security Classif. (of this report) Unclassified	20. Security Classif. (of this page) Unclassified	21. No. of Pages 30	22. Price \$0.00

Executive Summary

Vehicle emissions are major contributors to urban air pollution. Among many emission estimation methods and mitigation strategies, near-road air quality measurements serve as a fundamental method to understand the impact of the traffic emissions on ambient air quality and public health. In this project, we are particularly interested in utilizing near-road measurement data to analyze the impact of traffic, weather, and spatial parameters on the air quality in the near-road microenvironments.

In this study, we obtained fine particulate matter (PM_{2.5}) and nitrogen dioxide (NO₂) measurement data (5-minute average) from two near-road air monitoring stations (AMSs) managed by the South Coast Air Quality Management District. The objective of this study was to examine the relationship between air quality and traffic and weather parameters. With air quality measurement spanning over 11 months, we attempted to gain a better understanding of the near-freeway air pollutant concentration, traffic speed, traffic flow, and weather parameters.

We applied both multiple linear regression (MLR) and multivariate adaptive regression splines (MARS) models to examine the relationship among the weather conditions, traffic states, and near-freeway air pollutant concentrations. Both MLR and MARS showed that all weather parameters (e.g., relative humidity, temperature, wind) were significant variables. For the State Route 60 AMS, MLR gave the adjusted R² as 0.077 and 0.264 for PM_{2.5} and NO₂, respectively, and MARS gave the R² as 0.19 and 0.53, respectively. For the Interstate 710 AMS, MLR gave the adjusted R² as 0.035 and 0.324 for PM_{2.5} and NO₂, respectively, and MARS gave the R² as 0.11 and 0.62, respectively.

Generally, NO₂ concentration can be better explained by the selected variables than can PM_{2.5}. The test of traffic speed segmentation indicates that the traffic speed has a considerable influence on near-road pollutant concentrations. When applying MLR and MARS models for winter months, the prediction performance for PM_{2.5} improves significantly at both AMSs, but the improvement effect is moderate for NO₂. We recommend that controlling seasonal weather variables can significantly improve PM_{2.5} prediction performance.

Acknowledgments

We would like to thank Dr. Kanok Boriboonsomsin for his advice during the project. We also thank Mrs. Marcia Walker from the Texas A&M Transportation Institute for her administrative support throughout the project.

Table of Contents

List of Figures	viii
List of Tables	viii
Background and Introduction	1
Approach	1
Data Acquisition	2
Air Quality Data.....	2
Meteorological Data	3
Traffic Parameters	3
Data Preparation	4
Data Cleaning.....	4
Variable Transformation	5
Method	5
Multiple Linear Regression.....	5
Multivariate Adaptive Regression Splines.....	6
Results	6
Air Quality Data Visualization.....	6
Traffic Parameter Visualization	10
MLR Model Results.....	12
Traffic Speed Segmentation	14
MARS Model Results	15
Seasonal Fuel Blend Effects.....	18
Conclusions and Recommendations	19
Outputs, Outcomes, and Impacts	20
Research Outputs, Outcomes, and Impacts.....	20
Technology Transfer Outputs, Outcomes, and Impacts.....	20
Education and Workforce Development Outputs, Outcomes, and Impacts.....	20
References	21

List of Figures

Figure 1. (a) Illustration of the SCAQMD near-roadway AMS sites selected for this study; (b) street view of 60NR AMS; and (c) street view of 710NR AMS.....	3
Figure 2. Satellite images of the SCAQMD near-roadway AMSs selected for this study (source: Google Maps and PeMS).....	4
Figure 3. Histogram and Q-Q plot of PM _{2.5} before and after box-cox transformation with $\lambda = 0.5$	5
Figure 4. Calendar plot of 5-minute daily average PM _{2.5} /NO ₂ concentration at 60NR AMS (blank spaces in the middle of months mean missing data).....	7
Figure 5. Average PM _{2.5} concentration for each day of the week at 60NR AMS in June 2018.	8
Figure 6. Average NO ₂ concentration for each day of the week at 60NR AMS in June 2018.	8
Figure 7. Calendar plot of daily average PM _{2.5} /NO ₂ concentration at 710NR AMS.....	9
Figure 8. Average PM _{2.5} concentration for each day of the week at 710NR AMS in June 2018.	9
Figure 9. Average NO ₂ concentration for each day of the week at 710NR AMS in June 2018.	10
Figure 10. Aggregated traffic speed (mph) for each day of the week at SR-60 Postmile B in 2018.	11
Figure 11. Average traffic flow (vehicle/5 minute) for each day of the week at SR-60 Postmile B in 2018.	11
Figure 12. Aggregated traffic speed (mph) for each day of the week at I-710 Postmile B in 2018.	12
Figure 13. Average traffic flow (vehicle/5 minute) for each day of the week at I-710 Postmile B in 2018.	12
Figure 14. Predicted vs. observed graphs using the MLR model: (a) 60NR PM _{2.5} ; (b) 60NR NO ₂ ; (c) 710NR PM _{2.5} ; and (d) 710NR NO ₂	14
Figure 15. Predicted vs. observed graphs using the MARS model: (a) 60NR PM _{2.5} ; (b) 60NR NO ₂ ; (c) 710NR PM _{2.5} ; and (d) 710NR NO ₂	18

List of Tables

Table 1. Description of the Explanatory Variables for 60NR and 710NR.....	6
Table 2. List of Regression Coefficients for 60NR and 710NR MLR Analysis of PM _{2.5} and NO ₂	13
Table 3. MLR Adjusted R ² Values for 60NR and 710NR Speed Segment Results	15
Table 4. List of Basic Functions and the Associated Coefficients for MARS Analysis at 60NR AMS.....	16
Table 5. List of Basic Functions and the Associated Coefficients for MARS Analysis of PM _{2.5} and NO ₂ at 710NR AMS.....	17
Table 6. MLR and MARS Model R ² for All Data, Summer, and Winter Months	19

Background and Introduction

Vehicle emissions are major contributors to urban air pollution. Because of the continued growth of vehicle use and greater occurrence of traffic congestion, vehicle emissions are predicted to grow in the coming years (1, 2). Among many strategies of emission estimation and subsequent mitigation, near-road air quality measurements serve as a fundamental method to understand the impact of traffic emissions on ambient air quality and public health. Extensive near-road measurement studies have been performed for a variety of research purposes, including examining the relationship among near-road air pollutants, exposure, and health effects (3, 4, 5, 6) as well as evaluating the effects of traffic-calming strategies (7, 8, 9).

For this project, we were particularly interested in studies that utilized near-road measurement data to analyze the impact of traffic, weather, and spatial parameters on the air quality in the roadside or other microenvironments (2, 10, 11, 12, 13). For example, Zhang et al. (2) found that hard vehicle acceleration can lead to an increase of hydrocarbon (HC) and carbon monoxide (CO) emissions due to the fuel-rich mode, while deceleration can increase particulate matter (PM) and HC emissions due to unburned fuel. Based on a year-long roadside measurement campaign, Kimbrough et al. (13) revealed that although the average wind speed appeared to be an important explanatory factor, the monthly average traffic volume and frequency of downwind conditions were not enough to explain the monthly average excess in monthly CO concentrations. Bigazzi et al. (11) combined 20-second-interval freeway traffic data and in-vehicle ultrafine particulate (UFP) concentration data and found that traffic states had a small but significant impact on in-vehicle UFP and that vehicle ventilation was the dominant influence on in-vehicle UFP concentration.

In addition, near-road measurements can be applied to predict the near-road air quality or aggregated traffic emission factors based on models (14, 15, 16). For instance, Venkatram et al. (14) investigated near-road micrometeorology parameters and air quality measurements, with their dispersion model showing that the measured micrometeorology and air quality data agreed well with the predicted values. Choudhary and Gokhale (16) found that, during peak hour, emission factors of CO and HC were about four to seven times higher than during off-peak hours and that the emission factor of nitrogen oxides (NO_x) was about two times higher than that of the off-peak hour. Wu et al. (15) applied a multivariate adaptive regression splines model to mobile air quality measurements and traffic data and identified 11 traffic-related variables that had the most impacts on in-source PM concentration prediction.

In this study, we obtained fine PM (PM_{2.5}) and nitrogen dioxide (NO₂) measurement data (5-minute average) from two near-road air monitoring stations (AMSs) managed by the South Coast Air Quality Management District (SCAQMD). The object of this study was to examine the relationship between air quality and traffic and weather parameters. Using air quality measurements that spanned over 11 months, we attempted to gain better understanding of the near-freeway air pollutant concentration, traffic speed, traffic flow, and weather parameters.

Approach

We obtained 1-minute average concentrations of PM_{2.5} and NO₂ from two near-roadway AMSs managed by SCAQMD (17). The locations of the two stations are marked in Figure 1a, with street view images in Figure 1b and 1c. Figure 2 presents a more detailed image of each AMS in relationship to the traffic count data collected.

Data Acquisition

Air Quality Data

Air quality data were collected from two sites:

1. *Ontario SR-60 Near-Road (60NR) AMS*, located at 2330 S. Castle Harbour Place, Ontario, CA 91761. 60NR is approximately 10 m south of California State Route 60 (SR-60) between the Grove Avenue and Vineyard Avenue exits (Figure 2a). The monitoring station is equipped with a Horiba APNA 370 NO_x instrument for NO₂ measurements and a Thermo-Scientific 5014i for continuous PM_{2.5} measurements (18). This site was selected by SCAQMD because this location is known for its high traffic congestion during weekdays. The typical traffic mix is dominated by light-duty vehicles.
2. *Long Beach I-710 Near-Road (710NR) AMS*, located at 5895 Long Beach Boulevard, Long Beach, CA 90805. 710NR is located 20 m east of Interstate 710 (I-710) between the exits for W. Del Amo Boulevard and Long Beach Boulevard (Figure 2b). The monitoring station is equipped with a Thermo-Scientific 42i NO_x instrument for NO₂ measurements and a Thermo-Scientific 5014i for continuous PM_{2.5} measurements (19). This site was selected by SCAQMD because this location is known for having a significant amount of heavy-duty trucks accounting for the majority of freeway traffic.

The air quality data from the two AMSs were collected from January 2018 through November 2018. The 1-minute concentration values were then averaged to 5-minute values to match the time resolution of the traffic count data.

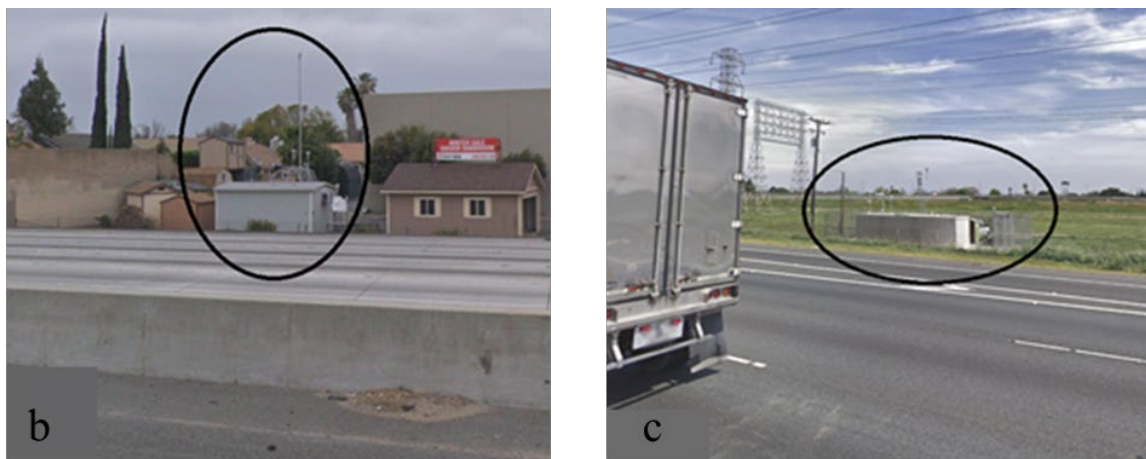


Figure 1. (a) Illustration of the SCAQMD near-roadway AMS sites selected for this study; (b) street view of 60NR AMS; and (c) street view of 710NR AMS.

Meteorological Data

Meteorological conditions are critical factors that influence ambient $PM_{2.5}$ and NO_2 concentration. The SCAQMD near-roadway AMS network also collects the following meteorological parameters: temperature, relative humidity, wind direction, and wind speed. The 1-minute meteorological data were collected from January 2018 through November 2018 and processed into 5-minute averaged data to match the time resolution of the traffic count data. We applied the arithmetic mean to concentration, humidity, and temperature. For wind speed and wind direction, the vector average method was used (20).

Traffic Parameters

The traffic metrics used in this study were obtained from the Caltrans Performance Measurement System (PeMS) (21). PeMS receives real-time 30-second raw measurements on traffic count and lane occupancy from each inductive loop detector (ILD) throughout the California freeway system. The system detects missing and invalid data and will correct the wrong values or fill in the missing data (22). Based on the traffic count and lane occupancy data for each lane, PeMS estimates an aggregated traffic speed at each ILD using the G-factor algorithm (23). Raw data are aggregated at different temporal levels (e.g., per 5 minutes, hourly, daily) in PeMS. PeMS also records the latitude and longitude of each vehicle detection station (VDS) and the corresponding postmile. Using

the PeMS “Station Metadata” and the nearest postmiles (Figure 2), we identified the nearest upstream and downstream VDS along both directions for both of the near-roadway AMSs. This study extracted the station-level 5-minute aggregated data, including flow and speed at both directions and at both postmiles. Due to data limitation, 1-hour truck vehicle miles traveled (VMT) on the road section near the AMS was applied as the surrogate of 5-minute truck flow and repeated 12 times for each hour. Data processing is discussed in the next section.



Note: (a) The SCAQMD site (red marker) adjacent to SR-60 and the corresponding postmiles (blue markers). Postmile A corresponds to PeMS abs Postmile 36.32 for SR-60 eastbound and PeMS abs Postmile 36.31 for SR-60 westbound. Postmile B corresponds to PeMS abs Postmile 37.65 for SR-60 eastbound and PeMS abs Postmile 37.64 for SR-60 westbound. (b) The SCAQMD site (red marker) adjacent to I-710 and the corresponding postmiles (blue markers). Postmile A corresponds to PeMS abs Postmile 6.04 for I-710 northbound and PeMS abs Postmile 5.99 for I-710 southbound. Postmile B corresponds to PeMS abs Postmile 7.17 for I-710 northbound and PeMS abs Postmile 6.93 for I-710 southbound. For both AMSs and each direction, Postmile A corresponds to the “Far-from-AMS” (Far) postmile, and B corresponds to the “Near-AMS” (Near) Postmile.

Figure 2. Satellite images of the SCAQMD near-roadway AMSs selected for this study (source: Google Maps and PeMS).

Data Preparation

Data Cleaning

The raw database obtained from near-road AMSs and PeMS required further data processing, including examining outliers, averaging values, and removing missing values.

All the data were within the reasonable range, and there were no detectable outliers. For 5-minute average values, the entry was labeled as null if more than 3 data points were missing within the 5 minutes.

After synchronizing 5-minute data for air pollutant concentration, traffic, and weather parameters, listwise deletion was applied to handle missing information; in other words, the row of data was removed if there were any null values (e.g., air pollutant concentration, traffic, or weather parameters) in the row. Since atmospheric pressure data were mostly missing, pressure values were excluded in the analysis for both stations.

Variable Transformation

Box-cox transformation was performed to transform abnormal concentration values to a normal-distribution shape (24). Lambda of 0.5 was applied for PM_{2.5} concentration (µg/m³), and the comparison of before and after transformation is presented in Figure 3. Before the transformation, the PM_{2.5} concentration distribution had a skewness of 1.501 (Figure 3a), and after the transformation, it conformed much better to a normal distribution, with a skewness of 0.235 (Figure 3b). The box-cox transformation did not improve NO₂ distribution and therefore was not applied to NO₂ concentration values.

The Pearson correlation coefficients were calculated to examine the linear relationship between any two numerical variables (25) to identify potential multicollinearity issues among the variables. The results indicated that the selected explanatory variables were not linearly related with each other.

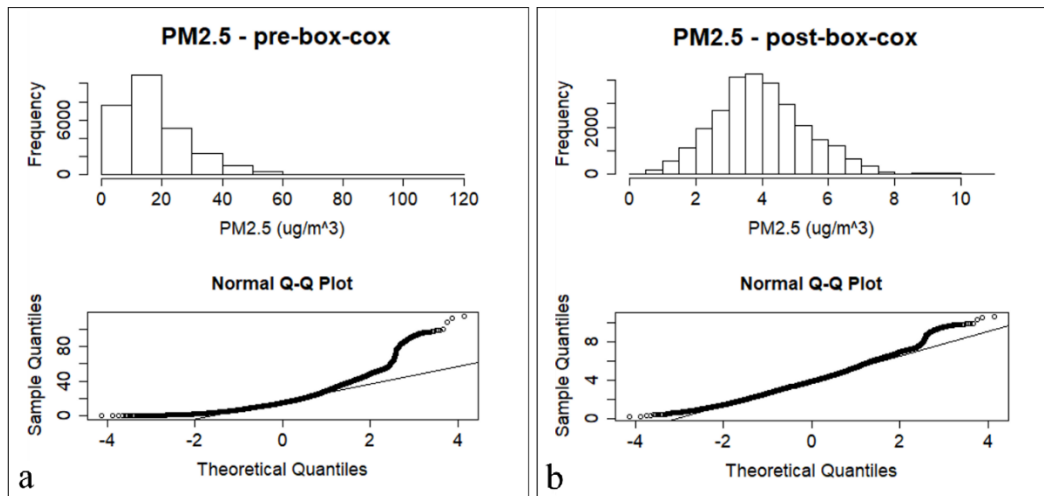


Figure 3. Histogram and Q-Q plot of PM_{2.5} before and after box-cox transformation with $\lambda = 0.5$.

Method

In this study, we visualized the air quality and traffic data based on various temporal scales to understand the fluctuation of the data. Further, two different regression models were applied to the database: (a) multiple linear regression (MLR), and (b) multivariate adaptive regression splines (MARS). All the regression models were performed using R version 3.5.1 (26).

Multiple Linear Regression

The MLR model is the simplest multivariate regression method that models the linear relationship between the explanatory variables on the observed traffic and meteorological parameters on PM_{2.5} and NO₂ concentrations. The general equation for the MLR model can be written as:

$$y = \beta_0 + \sum_i \beta_i * x_i + \varepsilon_i \quad (1)$$

where y represents the estimated model output; β_0 is the intercept; β_i is the regression coefficient associated with the i -th variable; x_i is the value of the i -th variable (Table 1); and ε_i is an independent, normally distributed, random error with zero mean and constant variance (27).

Table 1. Description of the Explanatory Variables for 60NR and 710NR

<i>i</i>	60NR	710NR	unit
0	Intercept		—
1	Relative Humidity		%
2	Temperature		Fahrenheit
3	Wind Speed		mph
4	Wind Direction		Degree
5	Speed West—Postmile A (Far)	Speed North—Postmile A (Far)	mph
6	Speed West—Postmile B (Near)	Speed North—Postmile B (Near)	mph
7	Speed East—Postmile A (Far)	Speed South—Postmile A (Far)	mph
8	Speed East—Postmile B (Near)	Speed South—Postmile B (Near)	mph
9	Flow West—Postmile A (Far)	Flow North—Postmile A (Far)	Vehicle/5 minutes
10	Flow West—Postmile B (Near)	Flow North—Postmile B (Near)	Vehicle/5 minutes
11	Flow East—Postmile A (Far)	Flow South—Postmile A (Far)	Vehicle/5 minutes
12	Flow East—Postmile B (Near)	Flow South—Postmile B (Near)	Vehicle/5 minutes
13	Weekly Timestamp		—
14	Truck VMT W	Truck VMT N	mph (applied as 5 minutes)
15	Truck VMT E	Truck VMT S	mph (applied as 5 minutes)

Multivariate Adaptive Regression Splines

To further explore the impacts of selected variables, a nonparametric regression technique, the MARS model (28), was also applied to the dataset used in this study. Even though the statistical properties of the resulting estimators are more difficult to determine, compared to the MLR model, the nonparametric regression techniques require fewer assumptions and can provide a better fit than the parametric techniques. The following description of MARS references Wu et al. (15). The MARS model can also be considered as an extension of the linear models that automatically capture nonlinearities and interactions using the following equation:

$$f(x) = \sum_i c_i * B_i(x) \quad (2)$$

where $f(x)$ is the estimated model output; and $B_i(x)$ is the i -th basis function that can be a constant 1, a hinge function, or a product of two or more hinge functions. When using the hinge function, it can take the form:

$$\max(0, x - const.) \quad (3)$$

or

$$\max(0, const. - x) \quad (4)$$

and automatically partition the input data so that the effects of any outliers can be attenuated. The MARS model tends to have a good bias-variance tradeoff due to the flexible but sufficiently constrained form of the basic functions to model nonlinearity with relatively low bias and variance.

Results

Air Quality Data Visualization

We plotted $PM_{2.5}$ and NO_2 concentrations at both stations based on several temporal scales—for example, the 5-minute daily average from January to November, as shown in Figure 4. We also plotted the calendar view of daily average traffic volume, and we found that the road section near the 710NR station had undergone a 3-month road closure from January to March in 2018. The road closure event greatly impacted the traffic pattern and may have involved heavy-duty off-road equipment and excessive road dust that might interfere with the air quality data.

Therefore, in the subsequent analysis, we removed data from January 1 to March 16 from the 710NR station’s dataset.

In consideration of the removed and missing data, we chose June as a representative month to present average concentration for each day of the week, and average concentration for each hour of the day, as displayed in Figure 4, Figure 5, and Figure 6.

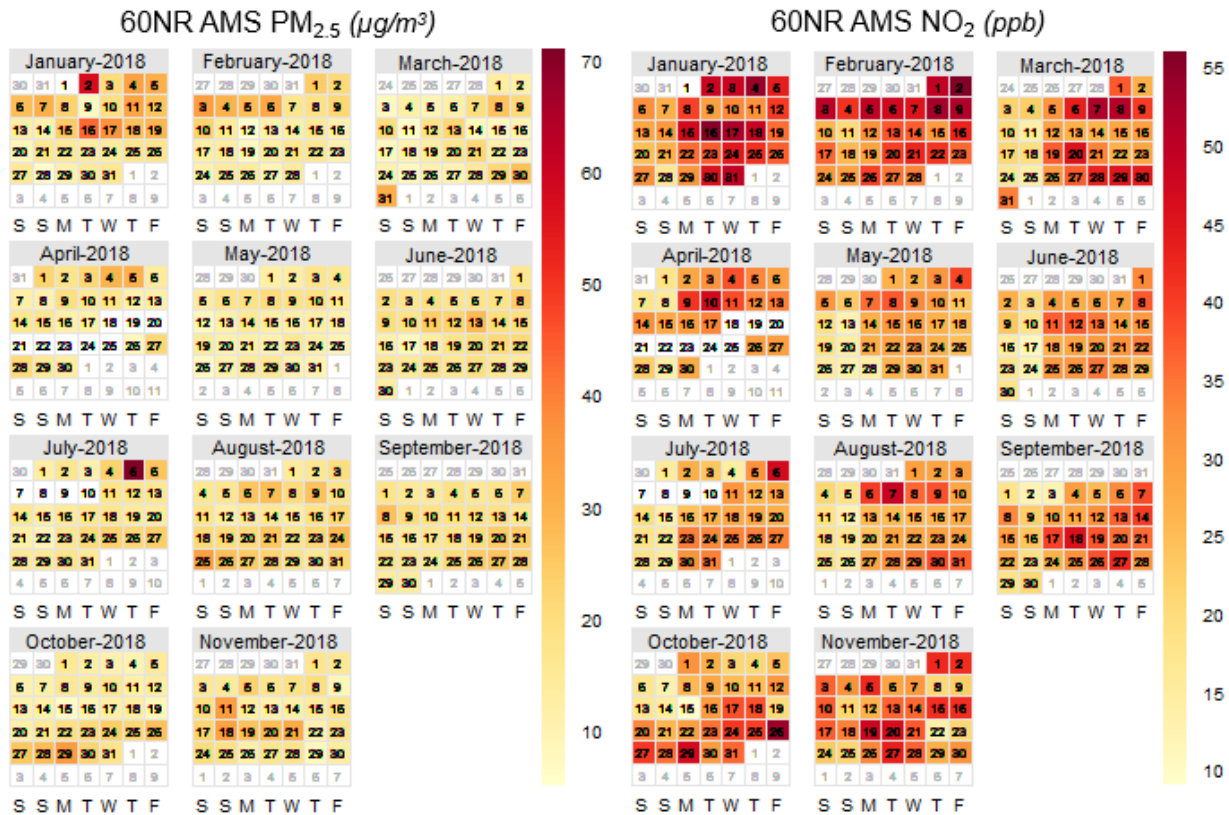


Figure 4. Calendar plot of 5-minute daily average PM_{2.5}/NO₂ concentration at 60NR AMS (blank spaces in the middle of months mean missing data).

Figure 4 reveals that the high PM_{2.5} concentration is more related to individual events (e.g., New Year’s Eve, July Fourth, etc.) rather than any specific pattern from day to day. In contrast, the NO₂ concentration presents a noticeable difference between most weekdays and weekends—the daily average NO₂ concentration is generally higher on weekdays and lower on weekends. This pattern can also be observed in Figure 5 and Figure 6.

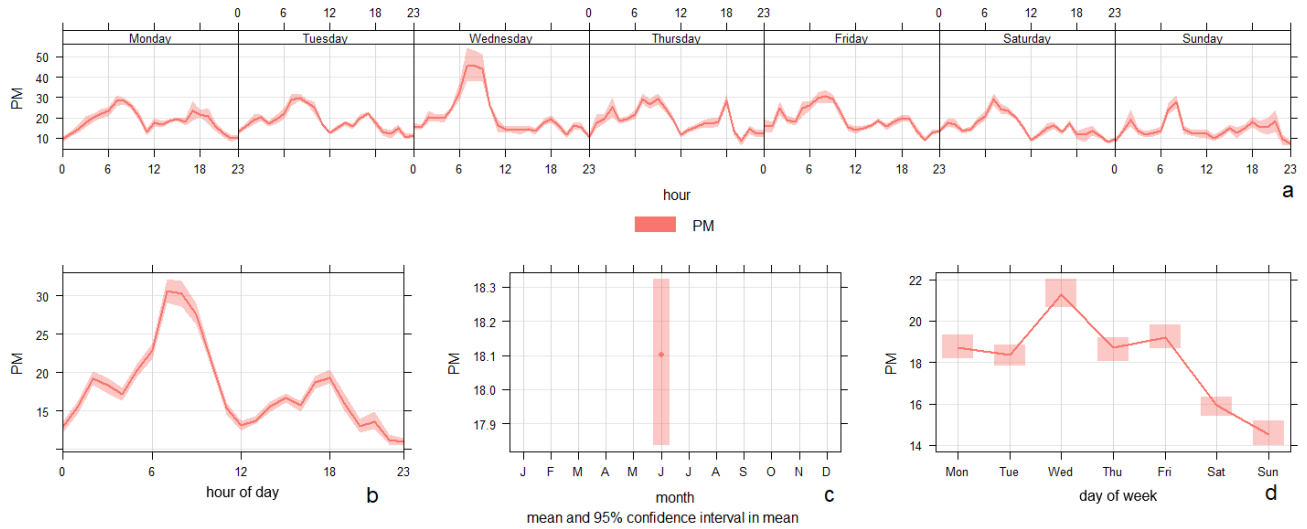


Figure 5. Average PM_{2.5} concentration for each day of the week at 60NR AMS in June 2018.

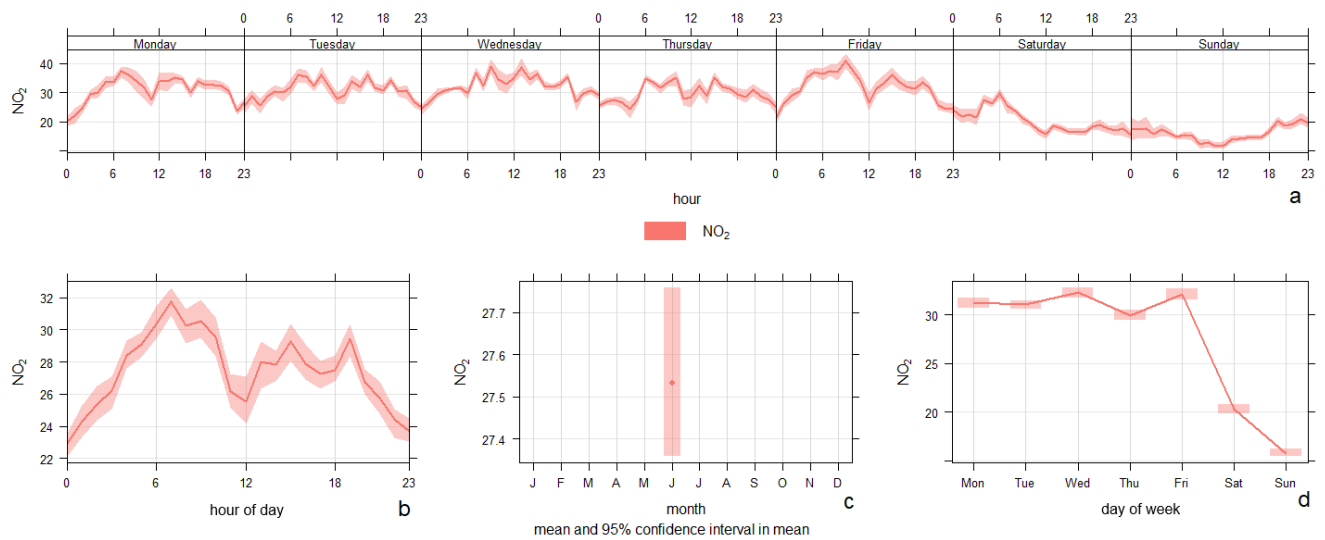


Figure 6. Average NO₂ concentration for each day of the week at 60NR AMS in June 2018.

Figure 5a displays the average concentration for each hour of the day on each day of the week. Figure 5b averages the concentration for each hour of the day for the entire month of June. Figure 5c shows the monthly average with a 95 percent confidence interval. Figure 5d shows daily average for each day of the week. The meaning of the subfigures also applies to Figure 6, Figure 8, and Figure 9. Figure 5d reveals a decreased PM_{2.5} concentration on weekends when compared with weekdays at the monthly average scale. However, the magnitude of decrease is much smaller than that of the NO₂ concentration shown in Figure 6.

The 710NR station shows a pattern similar to the 60NR station—the high PM_{2.5} concentration is more related to individual events (e.g., New Year’s Eve) and does not show much of a specific pattern from day to day. In contrast, the NO₂ concentration presents a noticeable difference between most weekdays and weekends.

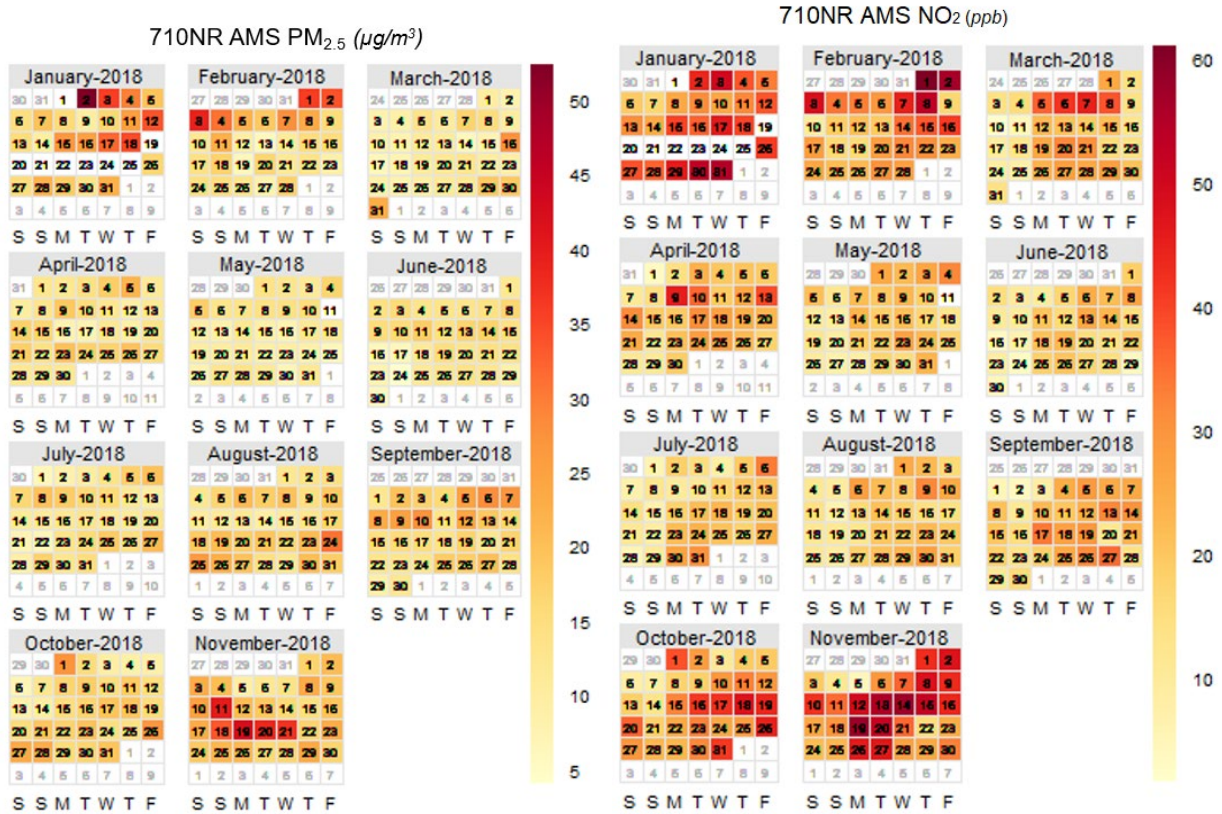


Figure 7. Calendar plot of daily average PM_{2.5}/NO₂ concentration at 710NR AMS.

As mentioned in Section 4.1, data from January 1 to March 16 at the 710NR station were removed due to a road closure event. In consideration of the removed and missing data, we chose June as a representative month to present average concentration for each day of the week and average concentration for hour of the day, as displayed in Figure 8 and Figure 9.

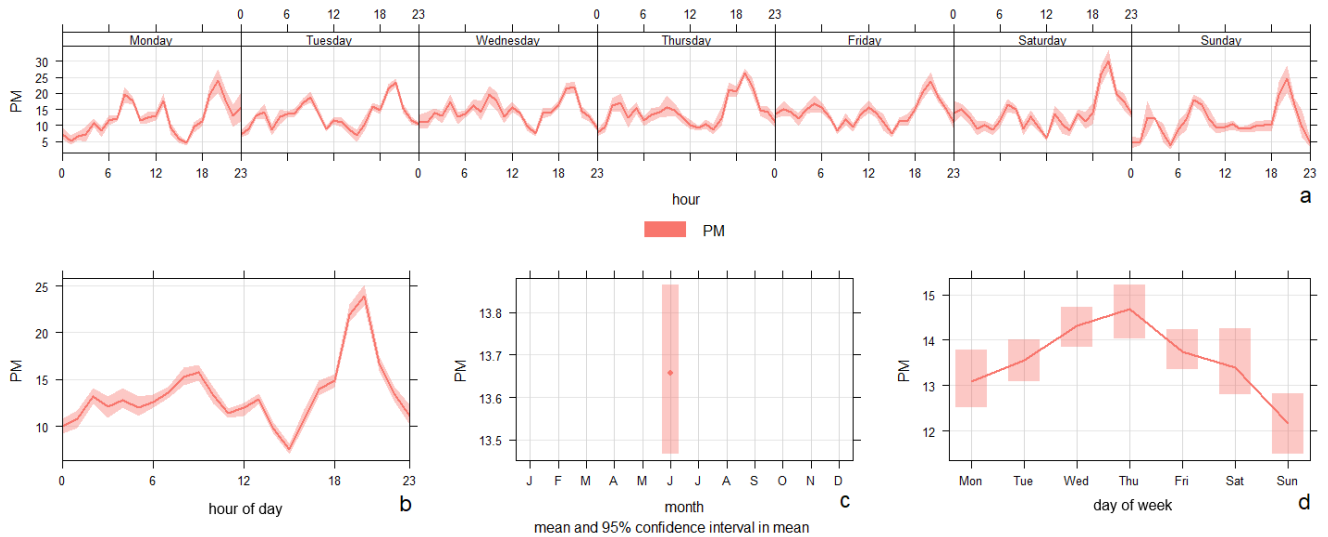


Figure 8. Average PM_{2.5} concentration for each day of the week at 710NR AMS in June 2018.

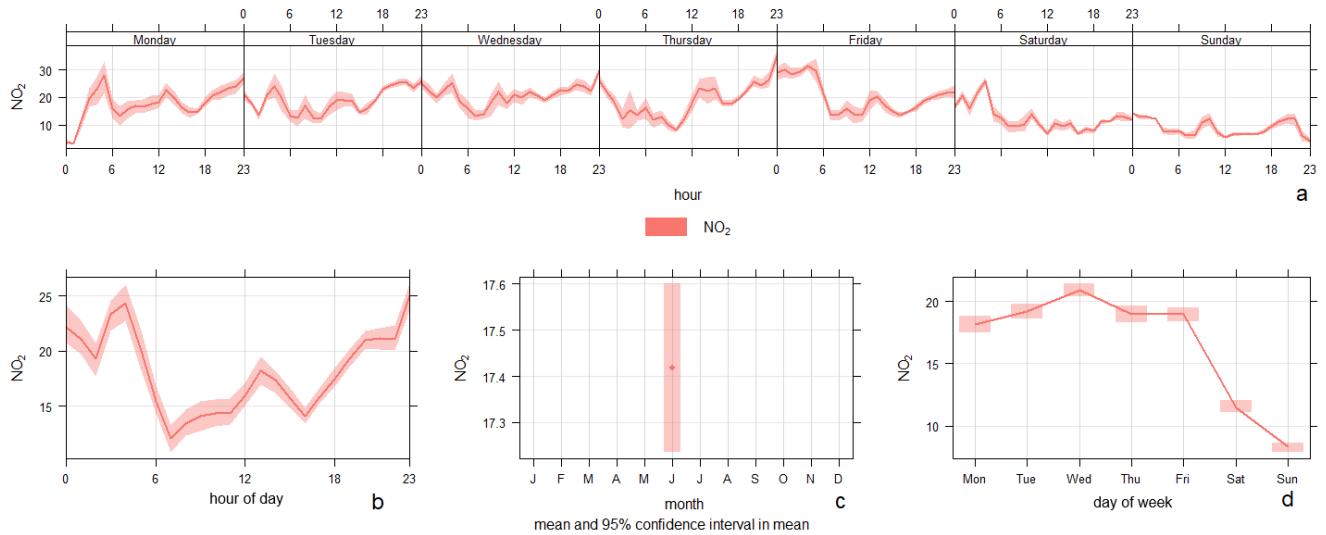


Figure 9. Average NO₂ concentration for each day of the week at 710NR AMS in June 2018.

Figure 8d depicts a slight decrease of average PM_{2.5} concentration on weekend days compared to that of weekdays. The average daily PM_{2.5} concentration for each day of the week (Figure 8d) does not fluctuate much, ranging from 12 to 15 μg/m³. Similar to the 60NR station, the weekend effects are more pronounced for NO₂ concentration than that of PM_{2.5} at the 710NR station. We attribute the different patterns of NO₂ and PM_{2.5} to their secondary formation from major sources—during the weekday, traffic contributes to a majority of ambient NO, which is quickly photolyzed to NO₂ (NO has a noontime lifetime of about 5 seconds) (29). Therefore, NO is photolyzed to NO₂ by the time it reaches the sensors, so decreased traffic volume may have led to reduced NO₂ levels. On the other hand, a large portion of ambient PM_{2.5} is from secondary formation and may take hours depending on the chemical compounds, which makes PM_{2.5} levels more independent from traffic parameters than NO₂. This finding is in line with the latest near-road research as well. For example, Seagram et al. analyzed 56 near-road NO₂ monitor stations and 31 PM_{2.5} near-road monitor stations. They found that annual mean PM_{2.5} concentrations at the NR stations have little correlation with annual average daily traffic (AADT), although there is some evidence that annual mean NO₂ concentrations increase with increasing AADT and fleet-equivalent AADT (30).

Figure 5b and Figure 6b for the 60NR station show that both PM_{2.5} and NO₂ concentrations undergo a continuous decrease from 7 a.m. to 12 p.m. However, this effect is not seen in Figure 8b and Figure 9b. A possible reason is that the 60NR station is located inland, where surface temperature as well as other local meteorological conditions change rapidly and lead to the continuous decrease. In contrast, the 710NR station is near the ocean, so the temperature changes are milder than those at the 60NR station, and the truck volume on I-710 is much larger than on SR-60. In summary, there are many factors that contribute to the similar and different patterns of both air pollutants at the two near-road AMSs. In the next section, the traffic patterns are briefly discussed.

Traffic Parameter Visualization

In this section, we plot the aggregated traffic speed (miles per hour) and traffic flow (vehicles per 5 minutes) for January to November in several time scales similar to those scales in Figure 5. Figure 10a displays the aggregated traffic speed for each hour of the day on each day of the week, Figure 10b averages the traffic speed for each hour of the day for 11 months, Figure 10c shows the monthly average, and Figure 10d plots the daily average for each day of the week. Both west- and eastbound on SR-60 are included in the figures, and the semi-transparent bars mark the 95 percent confidence interval. Figure 11 plots the traffic flow at similar temporal scales as those in Figure 10.

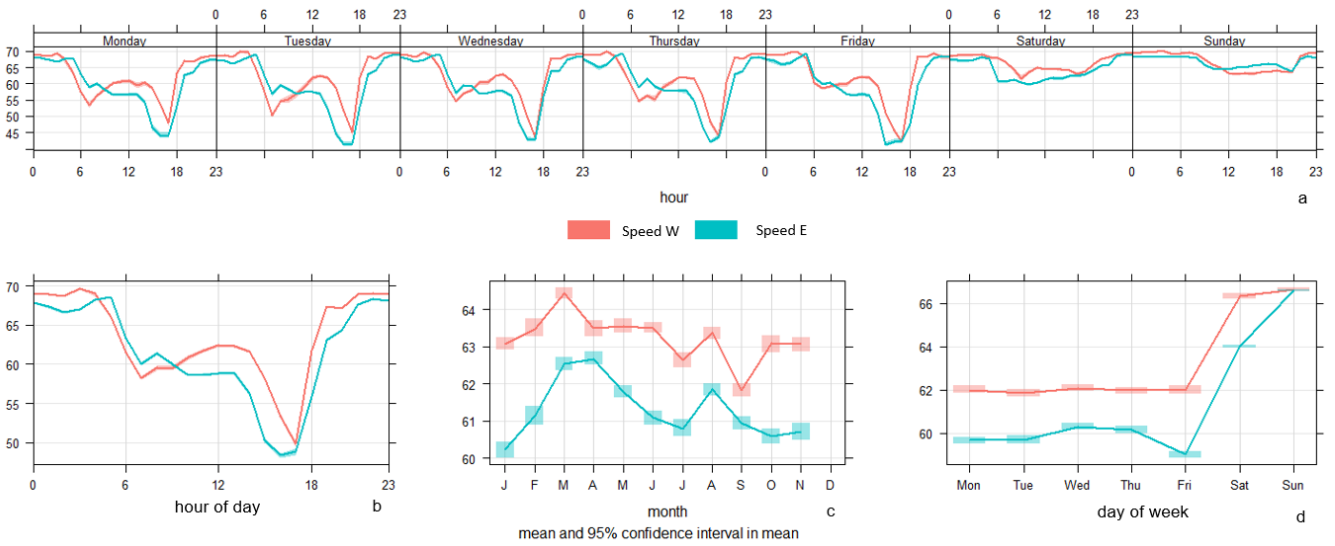


Figure 10. Aggregated traffic speed (mph) for each day of the week at SR-60 Postmile B in 2018.

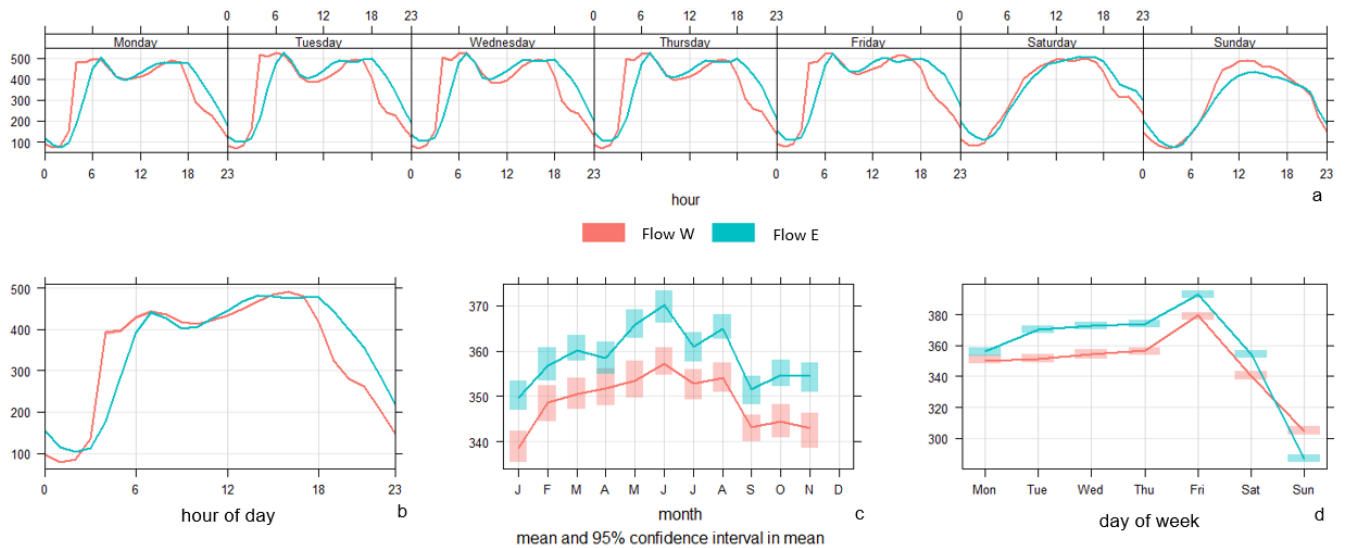


Figure 11. Average traffic flow (vehicle/5 minute) for each day of the week at SR-60 Postmile B in 2018.

From Figure 10a/b and Figure 11a/b, we observe a clear traffic pattern designating the morning peak at around 7 a.m. and the afternoon peak at around 5 p.m. on weekdays for both directions. For SR-60, both west- and eastbound traffic are mostly synchronized.

For I-710, as shown in Figure 12a/b and Figure 13a/b, the southbound shows a morning peak, while the northbound shows an afternoon peak. Note that the truck traffic on I-170 is significantly larger than that on SR-60. As mentioned in Section 2.1.3, 1-hour truck VMT on the road section near the AMS was applied as the surrogate of 5-minute truck flow. The average 1-hour truck VMT on SR-60 is 86 and 210 for east- and westbound traffic, respectively. On I-710, truck VMT is 907 and 807 for north- and southbound traffic, respectively. In the subsequent MLR and MARS model analysis, we examine the impact of the selected traffic parameters on the concentrations of near-road air pollutants.

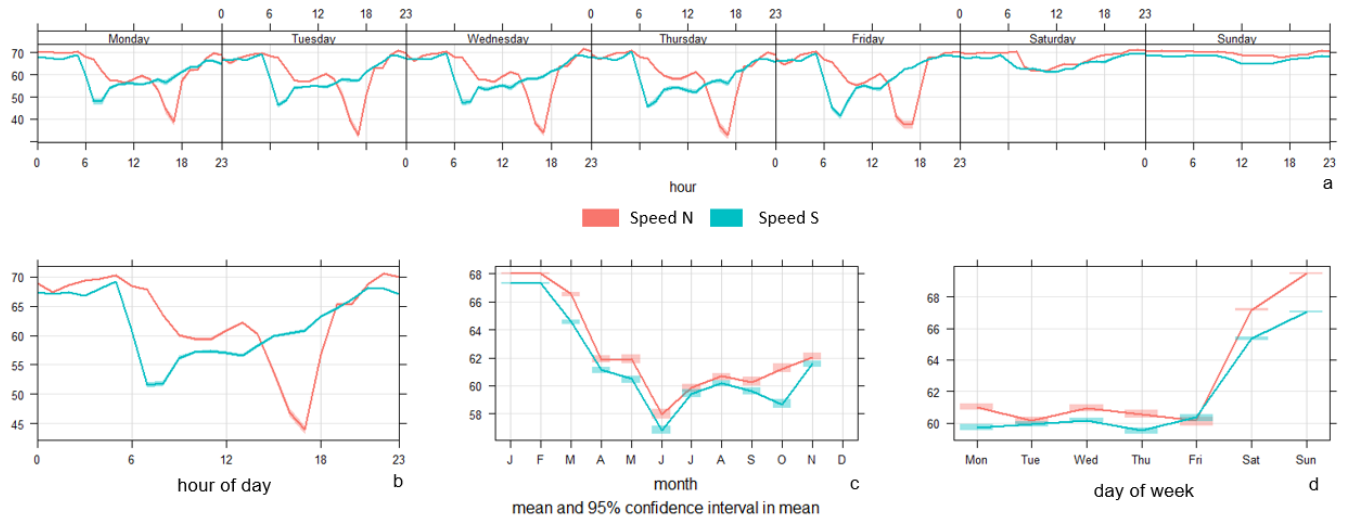


Figure 12. Aggregated traffic speed (mph) for each day of the week at I-710 Postmile B in 2018.

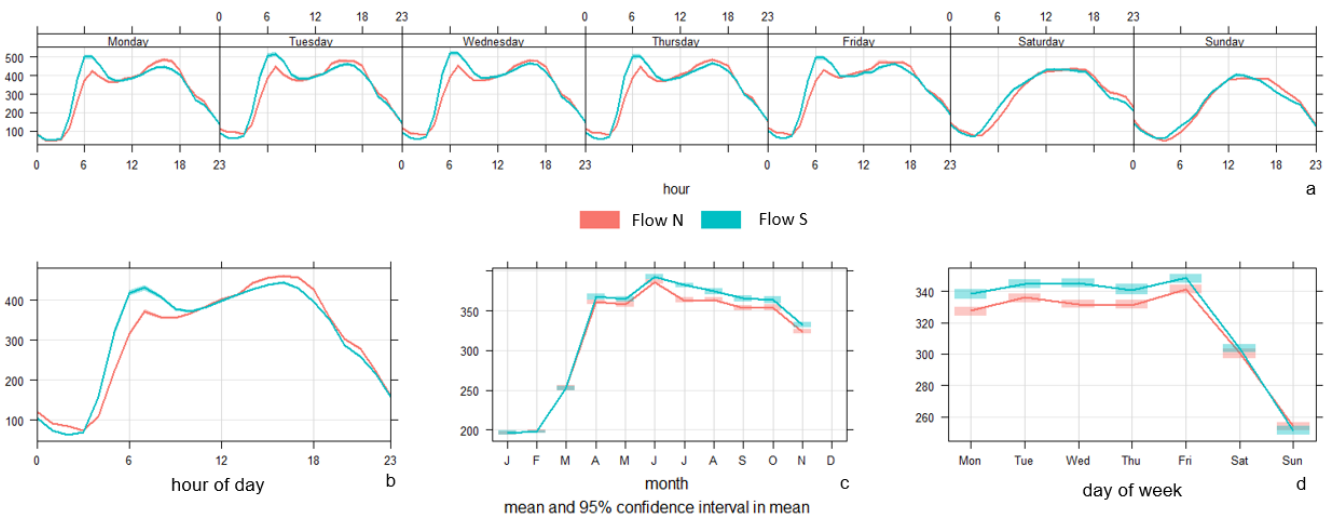


Figure 13. Average traffic flow (vehicle/5 minute) for each day of the week at I-710 Postmile B in 2018.

MLR Model Results

The results of MLR analyses for NO_2 and $\text{PM}_{2.5}$, measured from the two near-roadway AMSs, are shown in Table 2. At the 60NR AMS, the results indicated that for both $\text{PM}_{2.5}$ and NO_2 , all the weather parameters were significant at the 5 percent α -level. Relative humidity and temperature were positively related to $\text{PM}_{2.5}$ concentration; however, both were negatively related to NO_2 concentration. Wind direction was negatively related to both pollutants' concentration at the 60NR station, but the opposite was true for the 710NR station. Wind speed was positively related to both pollutant concentrations at both stations, and its coefficient's magnitude was largest among all weather parameters, indicating that wind speeds are more impactful than other weather factors.

Table 2. List of Regression Coefficients for 60NR and 710NR MLR Analysis of PM_{2.5} and NO₂

	SR-60				I-710			
	PM _{2.5}		NO ₂		PM _{2.5}		NO ₂	
	β_i	p-value	β_i	p-value	β_i	p-value	β_i	p-value
Intercept	2.80E+00	< 2e-16	8.03E+01	< 2e-16	2.83E+00	< 2e-16	4.93E+01	< 2e-16
RH	7.54E-03	< 2e-16	-1.61E-01	< 2e-16	8.48E-03	< 2e-16	-2.56E-01	< 2e-16
Temperature	1.15E-02	< 2e-16	-2.03E-01	< 2e-16	5.88E-03	5.48E-13	-4.89E-01	< 2e-16
Wind Speed	3.29E-01	< 2e-16	3.62E+00	< 2e-16	2.44E-01	< 2e-16	5.71E+00	< 2e-16
Wind Direction	-1.85E-03	< 2e-16	-2.81E-02	< 2e-16	5.36E-04	6.86E-12	5.25E-02	< 2e-16
Speed W/N - Postmile A (Far)	1.28E-02	0.213121	8.87E-02	0.338	-3.38E-02	0.0601	3.42E+00	< 2e-16
Speed W/N Postmile B (Near)	-1.06E-01	< 2e-16	-1.49E+00	< 2e-16	-3.64E-03	0.7302	-2.18E+00	< 2e-16
Flow W/N Postmile A (Far)	-8.28E-04	7.71E-12	1.75E-03	0.11	-1.14E-03	1.08E-10	-2.56E-02	< 2e-16
Flow W/N Postmile B (Near)	5.91E-04	2.28E-08	-1.31E-02	< 2e-16	7.56E-04	2.36E-05	-1.06E-02	3.44E-10
Speed E/S Postmile A (Far)	-3.92E-02	0.003232	-1.60E+00	< 2e-16	-1.52E-01	< 2e-16	-3.12E+00	< 2e-16
Speed E/S Postmile B (Near)	1.11E-01	5.42E-16	-8.94E-01	5.03E-13	1.13E-01	1.73E-14	2.46E+00	< 2e-16
Flow E/S Postmile A (Far)	-6.29E-04	0.000406	-7.70E-03	1.62E-06	3.04E-03	< 2e-16	4.12E-02	< 2e-16
Flow E/S Postmile B (Near)	2.03E-04	0.249995	1.06E-02	2.94E-11	-2.16E-03	< 2e-16	-2.41E-02	< 2e-16
Weekly Timestamp	5.19E-05	4.08E-11	2.02E-03	< 2e-16	4.34E-05	6.52E-06	2.14E-03	< 2e-16
Truck VMT W/N	1.75E-03	< 2e-16	1.73E-02	< 2e-16	3.44E-05	0.0375	6.22E-03	< 2e-16
Truck VMT E/S	9.40E-04	< 2e-16	3.36E-02	< 2e-16	5.12E-05	0.0125	2.67E-03	< 2e-16
Multiple R-squared	0.07675		0.2643		0.03475		0.3244	
Adjusted R-squared	0.07658		0.2641		0.03448		0.3242	
p-value	< 2.2e-16		< 2.2e-16		< 2.2e-16		< 2.2e-16	
Degrees of Freedom	80673		80673		52175		52175	
Residual Standard Error	1.242		11.21		1.236		11.69	

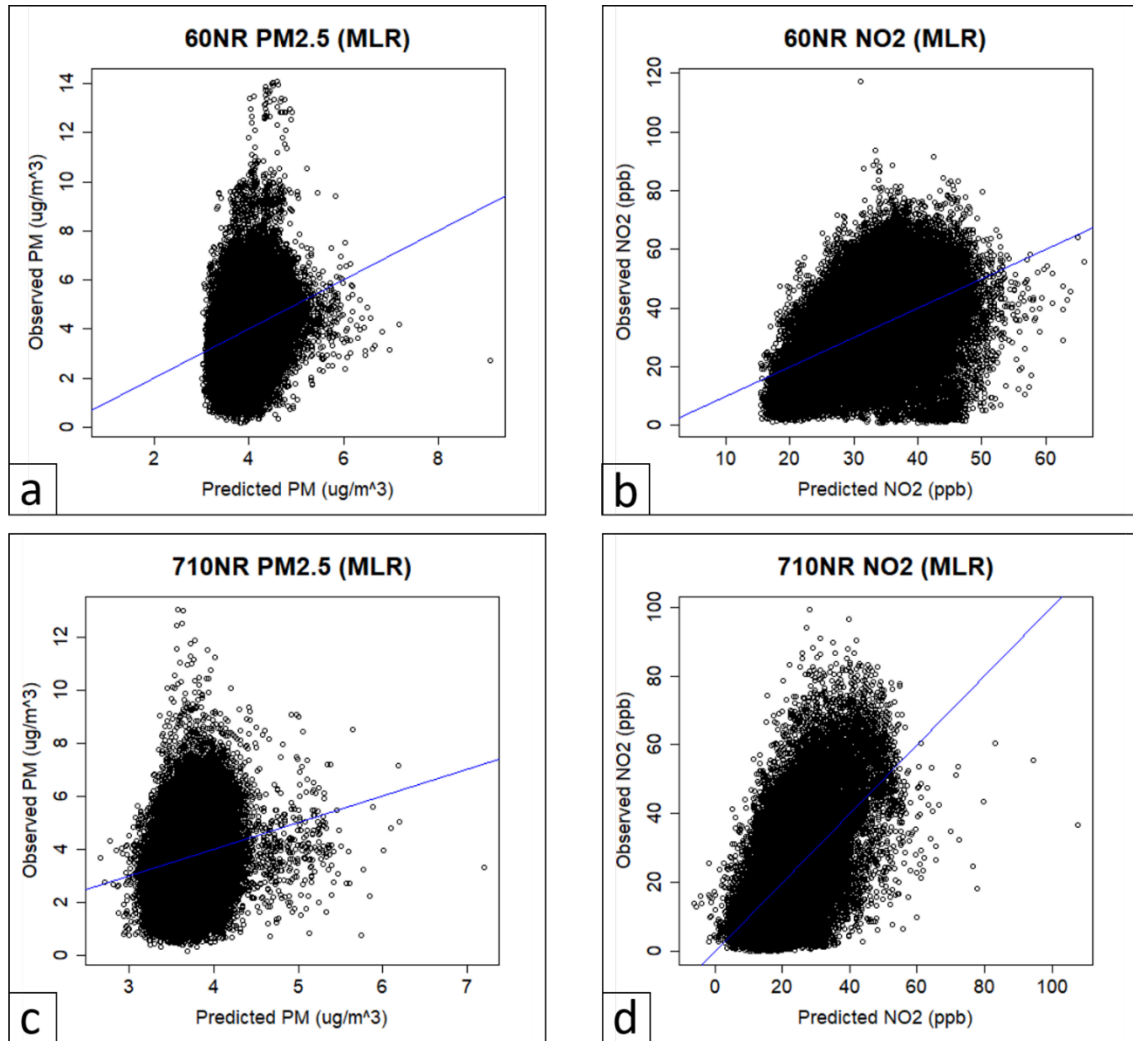
Note: Variables in boldface are statistically significant at the 5% α -level. Data from January 1 through March 16 were removed from 710NR due to a freeway closure event. For SR-60, the westbound direction is closer to the AMS. For I-710, the northbound direction is closer to the AMS. For any direction, Postmile B is closer to the AMS than Postmile A. Please refer to Figure 2.

At the 60NR station, westbound traffic speed at Postmile B (near) and eastbound traffic speed at both postmiles were significant for both pollutants. At the 710NR station, all traffic flow and speed parameters were significant for NO₂ concentration. A similar trend was found with PM_{2.5}, except that the northbound traffic speed at 710 was not significant. We found that at the 60NR AMS, the coefficients of west-direction (which is closer to the AMS) speed at Postmile B (closer to the AMS) were negative, which means that the higher the traffic speed is, the lower the pollutant concentration will be. On the other hand, the speed of the same direction at Postmile A (farther from the AMS) was not significant for either pollutants. At the 710NR AMS, the coefficient of the north-direction (which is closer to the AMS) speed at Postmile B (closer to the AMS) was negative for NO₂, but the same parameter was not significant for PM_{2.5}. However, the coefficients of traffic flow were not consistent at either station. At both stations, truck VMT was significant for both pollutants with a positive coefficient, which means that more trucks lead to higher pollutant concentration.

The adjusted R² values for NO₂ were much larger than the values of PM_{2.5}, indicating that NO₂ can be better explained by the explanatory variables than can PM_{2.5}. Our preliminary explanation for this finding is that on-road traffic contributes a large portion to the ambient primary NO, which will be quickly photolyzed into NO₂. On the other hand, a large percentage of PM_{2.5} comes from secondary formation; therefore, PM_{2.5} cannot be well explained by simultaneous traffic and weather factors.

The flow's influence on the pollutant concentration was not consistent and cannot be well explained since traffic volume and speed are not linearly related, similar speed could reflect different traffic volume/congestion levels, and traffic volumes could be quite different for each road direction at the same time. To further consider the impact of traffic speed, in the following sections, we apply segmented regression and MARS.

Figure 14 illustrates the comparison between observed and MLR-modeled NO_2 and $\text{PM}_{2.5}$ concentrations for both the 60NR and 710NR stations. We found that for $\text{PM}_{2.5}$, the range of values was from near zero to approximately $100 \mu\text{g}/\text{m}^3$ (since box-cox transformation was applied to $\text{PM}_{2.5}$, the original values are the square of that on the x- and y-axis), and a cluster of points stood outside of the point cloud. For NO_2 , the range of values was from near zero to approximately 70 ppb, and the cluster was tighter with fewer scattered points.



Note: Since box-cox transformation was applied to $\text{PM}_{2.5}$, the values on the x- and y-axis are the original values' square root.

Figure 14. Predicted vs. observed graphs using the MLR model: (a) 60NR $\text{PM}_{2.5}$; (b) 60NR NO_2 ; (c) 710NR $\text{PM}_{2.5}$; and (d) 710NR NO_2 .

Traffic Speed Segmentation

Due to the nonlinearity between traffic speed and volume, segmenting the traffic speed can help better understand the impact of traffic speed and volume. Three speed ranges were tested using the MLR model. As

shown in Table 3, for example, considering SR-60 westbound, we assumed that congestion would occur when all speeds became less than 30 mph at both postmiles, and free-flow status would return when all speeds were greater than or equal to 45 mph in the westbound direction, with no speed constraints for the eastbound direction. One transition range between 30 to 45 mph was considered. The numbers in parentheses represent the number of data rows in this speed range.

Table 3. MLR Adjusted R² Values for 60NR and 710NR Speed Segment Results

MLR model		SR-60				I-710			
adjusted R ² values		SR-60 West		SR-60 East		I-710 North		I-710 South	
(number of data points)		PM _{2.5}	NO ₂						
> 45 MPH	Free-Flow	0.07694	0.2882	0.07586	0.3025	0.03724	0.3551	0.05088	0.3735
		(72,603)	(72,603)	(71,998)	(71,998)	(46,892)	(46,892)	(43,859)	(43,859)
30 - 45 MPH	Transition	0.1185	0.1466	0.1312	0.1111	0.03647	0.3888	0.06585	0.5043
		(3,707)	(3,707)	(6,767)	(6,767)	(4,607)	(4,607)	(3,237)	(3,237)
< 30 MPH	Congestion	0.1379	0.1535	0.1036	0.1479	0.03215	0.4255	0.09963	0.4537
		(1,577)	(1,577)	(852)	(852)	(3,762)	(3,762)	(2,134)	(2,134)

Note: Green cells mark those adjusted R² values that are larger than the ones in Table 2.

We found that for I-710, segmenting speed improved for nearly all adjusted R² values compared to the values shown in Table 2, except for PM_{2.5} northbound in the range of congestion. For SR-60, R² values of PM_{2.5} improved in the congestion and transition range; on the other hand, R² values of NO₂ improved in the free-flow range. However, the improvements were slight for NO₂ and moderate for PM_{2.5}. One challenge or limitation of such an analysis is the need to characterize traffic states in both directions, which can be very different (e.g., traffic speed, total flow, and truck flow might vary significantly on north- and southbound lanes of a freeway) and have a combined influence on the near-road concentrations. In response to this limitation, measuring near-road CO₂ concentration can help quantify out-of-tailpipe traffic emissions, which can serve as an impactful surrogate in addition to existing traffic parameters.

MARS Model Results

In Table 4, the results for PM_{2.5} indicate that the important explanatory variables included all meteorological parameters—westbound traffic speed for Postmile B (closest to the AMS), eastbound traffic speed for Postmile A (farther from the AMS), and truck flow in both directions. For NO₂, the significant variables also included all the meteorological parameters—eastbound traffic speed for Postmile A (farther/downstream of AMS) and truck volume on the eastbound lanes. The weekly timestamp was significant for both pollutants.

The variable of importance and the values in the corresponding basic functions represent the associated values that are critical to the partitioning for that set of explanatory variables. For example, for PM_{2.5} (as shown in Table 4), 0.74 mph was a critical partitioning point for the wind speed values. The R² values were 0.19 for PM_{2.5} and 0.53 for NO₂, which were much improved compared to the values of the MLR model.

Table 4. List of Basic Functions and the Associated Coefficients for MARS Analysis at 60NR AMS

60NR			
PM _{2.5}		NO ₂	
c	β _i	c	β _i
Intercept	43.355016	Intercept	17.130823
max(RH-22.0705)	-0.066942	max(28.9611-RH)	-0.427762
max(36.2282-RH)	-0.095664	max(RH-28.9611)	-0.357562
max(RH-36.2282)	0.068511	max(80.0102-T)	0.365037
max(RH-93.2093)	-0.167041	max(T-80.0102)	0.22911
max(37.4461-T)	0.096897	max(0.56077-WS)	-52.210679
max(T-37.4461)	0.026512	max(WS-0.56077)	13.867884
max(0.739848-WS)	-2.006632	max(WS-0.835207)	-12.999226
max(WD-95.2485)	-0.009671	max(WD-51.1709)	0.285913
max(WD-202.809)	0.006859	max(WD-105.405)	-0.289689
max(287.111-WD)	-0.001935	max(WD-216.329)	0.238612
max(WD-287.111)	0.015549	max(WD-241.484)	-0.450622
max(8.11172-Speed West_Postmile B Near)	0.105193	max(WD-292.524)	0.579614
max(Speed West_Postmile B Near)-8.11172)	0.275016	max(305.89-WD)	0.071572
max(Speed East_Postmile A Far-7.7846)	-0.317208	max(WD-305.89)	-0.243614
max(658-Weekly Timestamp)	-0.000498	max(8.18535-Speed East_Postmile A Far)	2.703334
max(Weekly Timestamp-658)	-0.00004	max(786-Weekly Timestamp)	-0.012033
max(Truck VMT W-26.4)	-0.113277	max(Weekly Timestamp-786)	-0.000492
max(137.4-Truck VMT W)	-0.110027	max(Weekly Timestamp-1646)	-0.03758
max(Truck VMT W-137.4)	0.11419	max(Weekly Timestamp-1871)	0.08592
max(Truck VMT E-6.7)	-0.146963	max(82.4-Truck VMT E)	-0.098167
max(179.3-Truck VMT E)	-0.146638		
max(Truck VMT E-179.3)	0.149305		
R-squared: 0.1904561		R-squared: 0.5312249	

Note: RH = relative humidity; WS = wind speed; WD = wind direction. Variables in boldface are statistically significant at the 5% α-level. Data from January 1 through March 16 were removed from 710NR due to a freeway closure event. For SR-60, the westbound direction is closer to the AMS. For I-710, the northbound direction is closer to the AMS. For any direction, Postmile B is closer to the AMS than Postmile A. Please refer to Figure 2.

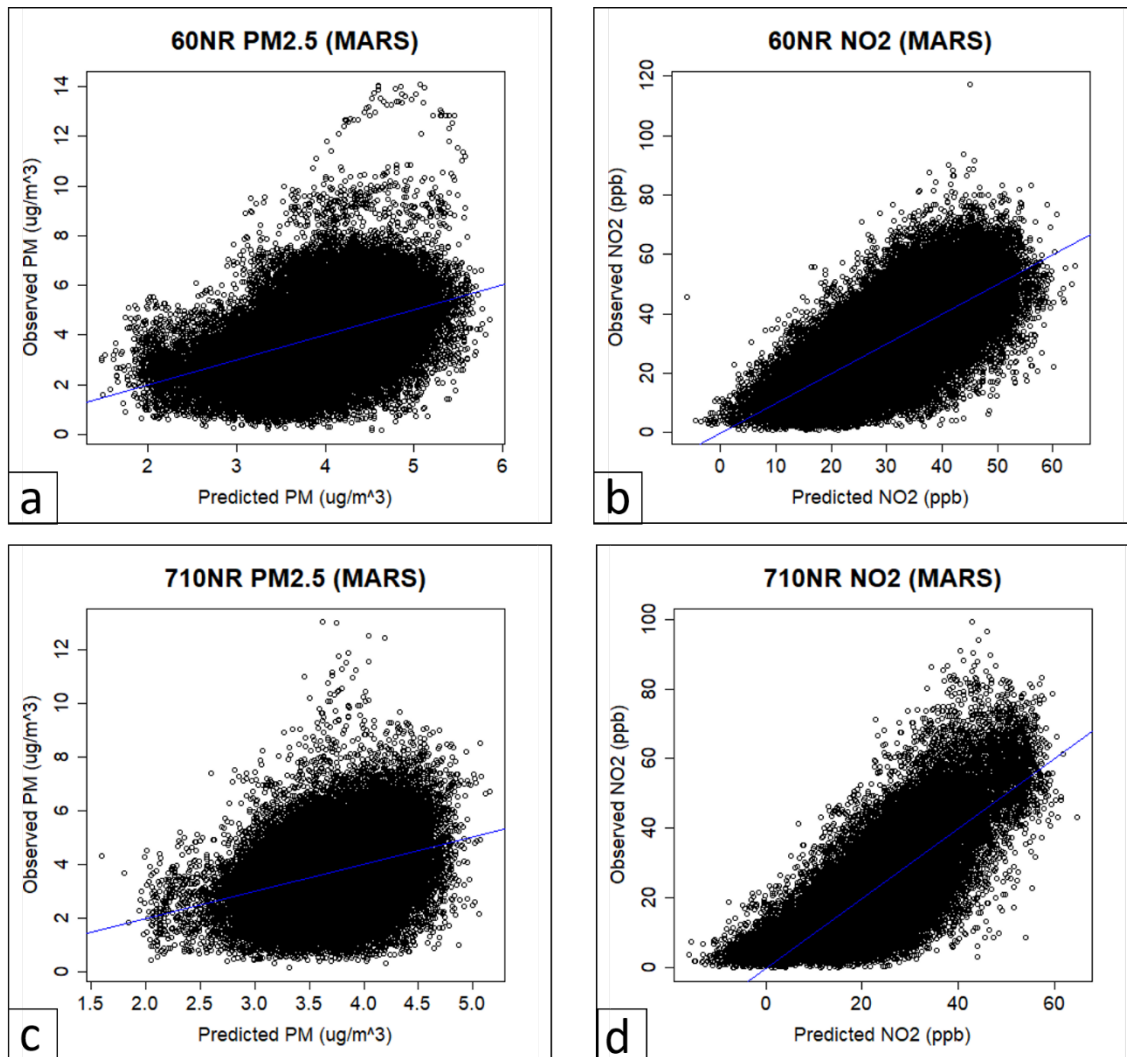
Similar to the MARS results at the 60NR AMS and previous MLR results, all the meteorological parameters were important variables for near-road concentrations. For the traffic parameters, Table 5 shows that the variables of importance were northbound traffic speed at Postmile A (farther from the AMS), southbound speed at both postmiles, and southbound flow at both postmiles for PM_{2.5}. For NO₂, except for southbound traffic speed and volume at Postmile B (closer to the AMS), all other variables were significant. Therefore, the northbound traffic conditions, which the AMS is directly next to, always play an important role in the near-road pollutant concentration. The R² values were 0.11 for PM_{2.5} and 0.62 for NO₂, respectively. When comparing the MARS results for NO₂ (Table 4 and Table 5), 710NR had a higher R² value than 60NR. When comparing the MARS results for PM_{2.5} (Table 4 and Table 5), the R² value for the 60NR was higher than the value of 710NR. The comparisons are consistent with observations based on the MLR results.

Table 5. List of Basic Functions and the Associated Coefficients for MARS Analysis of PM_{2.5} and NO₂ at 710NR AMS

I710			
PM_{2.5}		NO₂	
c	β _i	c	β _i
Intercept	3.1635616	Intercept	310.184339
max(30.2091-RH)	-0.0473251	max(RH-8.79354)	-4.153581
max(RH-30.2091)	0.003585	max(79.1806-RH)	-3.848194
max(64.7211-T)	0.0355646	max(RH-79.1806)	4.154356
max(T-64.7211)	0.0234869	max(71.8221-T)	0.452492
max(0.478509-WS)	-4.1550809	max(T-71.8221)	-0.036345
max(WS-0.478509)	1.0825181	max(0.642452-WS)	-57.81688
max(WS-0.824119)	-1.0302907	max(WS-0.642452)	7.111035
max(136.504-WD)	0.0031257	max(WS-1.24702)	-6.32268
max(WD-136.504)	0.0019277	max(116.093-WD)	0.139704
max(7.93725-Speed North_Postmile A Far)	0.0882385	max(WD-116.093)	-0.035096
max(Speed North_Postmile A Far-7.93725)	-0.5610164	max(WD-160.074)	0.284674
max(8.11788-Speed South_Postmile A Far)	0.0945724	max(WD-244.785)	-0.386951
max(Speed South_Postmile A Far-8.11788)	-0.6947021	max(WD-275.257)	0.148825
max(7.42967-Speed South_Postmile B Near)	0.1067995	max(7.38918-Speed South_Postmile A Far)	1.203326
max(Speed South_Postmile B Near-7.42967)	0.6204591	max(Speed South_Postmile A Far-7.38918)	-8.721842
max(318-Flow South_Postmile A Far)	-0.0061712	max(7.16938-Speed South_Postmile B Near)	0.810981
max(Flow South_Postmile A Far-318)	-0.000642	max(Speed South_Postmile B Near-7.16938)	8.967516
max(232-Flow South_Postmile B Near)	0.0054507	max(Weekly Timestamp-522)	-0.009979
max(Flow South_Postmile B Near-232)	-0.0007401	max(1485-Weekly Timestamp)	-0.011478
max(164.5-Truck VMT S)	-0.0033027	max(Weekly Timestamp-1485)	-0.004477
max(Truck VMT S-164.5)	0.000155	max(574.6-Truck VMT N)	-0.013503
		max(Truck VMT N-574.6)	0.00264
		max(209.9-Truck VMT S)	-0.022962
		max(Truck VMT S-209.9)	0.001861
R-squared: 0.1095426		R-squared: 0.6201496	

Note: RH = relative humidity; WS = wind speed; WD = wind direction. Variables in boldface are statistically significant at the 5% α-level. Data from January 1 through March 16 were removed from 710NR due to a freeway closure event. For SR-60, the westbound direction is closer to the AMS. For I-710, the northbound direction is closer to the AMS. For any direction, Postmile B is closer to the AMS than Postmile A. Please refer to Figure 2.

Figure 15 plots the comparison between observed and MARS-modeled NO₂ and PM_{2.5} concentrations for both 60NR and 710NR. Similar to the MLR model, the point cloud for PM_{2.5} was quite spread out but much improved when compared to Figure 14. On the other hand, the cluster of NO₂ points was tighter, with fewer scattered points. The overall prediction performance of MARS was better than the performance of MLR.



Note: Since box-cox transformation was applied to PM_{2.5}, the values on the x- and y-axis are the original values' square root.

Figure 15. Predicted vs. observed graphs using the MARS model: (a) 60NR PM_{2.5}; (b) 60NR NO₂; (c) 710NR PM_{2.5}; and (d) 710NR NO₂.

Seasonal Fuel Blend Effects

To examine the seasonal fuel blend effects, we utilized California's gasoline blend regulation to determine the months of summer and winter. California's Phase 2 Reformulated Gasoline (CaRFG2) and Phase 3 Reformulated Gasoline (CaRFG3) regulations require refiners to produce gasoline that meets eight specifications to reduce air pollution from the gasoline used in motor vehicles. One of the eight specifications is a standard for Reid vapor pressure, which is designed to reduce evaporative emissions during the summer months when ambient temperatures are their highest (31, 32).

According to the regulations, the summer fuel blend months for Southern California are April 1 through October 31, and winter fuel blend months are November 1 through March 31 of the next year. Therefore, we determined the summer and winter months based on the specified months of each fuel blend. We performed MLR and MARS models on the summer and winter months, and the results are summarized in Table 6.

Table 6. MLR and MARS Model R² for All Data, Summer, and Winter Months

R ²	SR-60		I-710	
	PM _{2.5}	NO ₂	PM _{2.5}	NO ₂
MLR all	0.077	0.264	0.035	0.324
MARS all	0.190	0.531	0.110	0.620
MLR Summer Months	0.086	0.275	0.026	0.270
MLR Winter Months	0.104	0.173	0.202	0.429
MARS Summer Months	0.166	0.527	0.094	0.597
MARS Winter Months	0.309	0.551	0.324	0.697

Note: Green cells mark those adjusted R² values that are larger than the results of MLR all. Blue cells mark those adjusted R² values that are larger than the results of MARS all.

We found that when applying models to winter months, the prediction performance for PM_{2.5} improved significantly. However, the improvement of applying winter months was moderate for NO₂. In contrast, applying the models to the summer season did not increase the R² or only led to slight improvements.

We examined the monitoring data from a regular AMS (Mt. Rubidoux Monitoring Station) within 10 mi of the 60NR station. We attempted to compare the pollutant concentration at the Mt. Rubidoux station to the concentration at the 60NR station, and we found that even though the concentration values at the Mt. Rubidoux station were generally smaller than the values at the 60NR station, including the values at the Mr. Rubidoux station as background values made the prediction performance much worse. Therefore, we did not further examine the background concentration. We believe that the correct background concentration will provide new insights on the contribution of mobile sources, especially for PM_{2.5}.

Conclusions and Recommendations

We applied both the MLR and MARS models to examine the relationship among the weather conditions, traffic states, and near-freeway air pollutant concentrations. Both the MLR and MARS models showed that all weather parameters (e.g., relative humidity, temperature, wind) were significant variables. For the SR-60 AMS, the MLR model gave the adjusted R² as 0.077 and 0.264 for PM_{2.5} and NO₂, respectively, and the MARS model gave the R² as 0.19 and 0.53, respectively. For the I-710 AMS, the MLR model gave the adjusted R² as 0.035 and 0.324 for PM_{2.5} and NO₂, respectively, and the MARS model gave the R² as 0.11 and 0.62, respectively.

We found that when applying models for winter months, the prediction performance for PM_{2.5} improved significantly. However, the improvement of applying winter months was moderate for NO₂. In contrast, applying models for the summer season did not increase the R² or only led to slight improvements.

To potentially explain the results, we refer to the air quality management plan released by SCAQMD every few years, which states, "Elevated PM₁₀ and PM_{2.5} concentrations can occur in the South Coast Air Basin throughout the year but occur most frequently in fall and winter. Although there are some changes in emissions by day-of-week and season, the observed variations in pollutant concentrations are primarily the result of seasonal differences in weather conditions" (33). Based on previous research, the latest near-road monitoring results, and our modeling analysis, we recommend that in addition to examining background concentration, controlling seasonal weather variables can potentially significantly improve PM_{2.5} prediction performance. Furthermore, in response to the limitation of characterizing traffic states in both directions, measuring near-road CO₂

concentration can help quantify out-of-tailpipe traffic emissions, which can serve as an impactful surrogate in addition to existing traffic parameters.

Outputs, Outcomes, and Impacts

Outputs: We demonstrate that controlling seasonal weather variables can potentially improve PM_{2.5} and NO₂ prediction performance based on weather and traffic data.

Research Outputs, Outcomes, and Impacts

- Peer-reviewed publications.
 - Extended Abstract:

Moretti, Ayla, Ji Luo, Guoyuan Wu, Brandon Feenstra, Kanok Boriboonsomsin, and Matthew Barth. Understanding Air Quality Data, Traffic, and Weather Parameters Collected from Near-Road Stations. Transportation Research Board Annual Meeting. No. 19-03343. 2019.
- Presentations at conferences and technical meetings.
 - Poster Presentation:

Moretti, Ayla, Ji Luo, Guoyuan Wu, Brandon Feenstra, Kanok Boriboonsomsin, and Matthew Barth. Understanding Air Quality Data, Traffic, and Weather Parameters Collected from Near-Road Stations. Presented at Transportation Research Board Annual Meeting, No. 19-03343, Washington, D.C., January 2019; and at Center for Advancing Research in Transportation Emission, Energy, and Health Symposium, Austin, Texas, February 2019.

Technology Transfer Outputs, Outcomes, and Impacts

We processed datasets of 5-minute air quality, traffic, and meteorological parameters for 11 months in 2018. The data can serve as training samples for future air pollutant concentration modeling.

Education and Workforce Development Outputs, Outcomes, and Impacts

Ayla Moretti is the PhD candidate who has worked on this project. Ayla has been actively involved in data processing, statistical modeling, and R/MATLAB scripting and performed most of the work during the project. Ayla has also won the CARTEEH Student of the Year award and successfully presented the study at two conferences in 2019.

References

- 1 Smit, R., L. Ntziachristos, and P. Boulter. Validation of road vehicle and traffic emission models—a review and meta-analysis. *Atmospheric Environment*, Vol. 44, No. 25, 2010, pp. 2943–2953.
- 2 Zhang, K., S. Batterman, and F. Dion. Vehicle emissions in congestion: comparison of work zone, rush hour and free-flow conditions. *Atmospheric Environment*, Vol. 45, No. 11, 2011, pp. 1929–1939.
- 3 McCreanor, J., P. Cullinan, M. J. Nieuwenhuijsen, J. Stewart-Evans, E. Malliarou, L. Jarup, R. Harrington, M. Svartengren, I.-K. Han, and P. Ohman-Strickland. Respiratory effects of exposure to diesel traffic in persons with asthma. *New England Journal of Medicine*, Vol. 357, No. 23, 2007, pp. 2348–2358.
- 4 McAuley, T. R., and M. Pedroso. *Safe Routes to School and Traffic Pollution: Get Children Moving and Reduce Exposure to Unhealthy Air*. 2012.
- 5 Weichenthal, S., M. Hatzopoulou, and M. S. Goldberg. Exposure to traffic-related air pollution during physical activity and acute changes in blood pressure, autonomic and micro-vascular function in women: a cross-over study. *Particle and Fibre Toxicology*, Vol. 11, No. 1, 2014, p. 70.
- 6 Sinharay, R., J. Gong, B. Barratt, P. Ohman-Strickland, S. Ernst, F. J. Kelly, J. J. Zhang, P. Collins, P. Cullinan, and K. F. Chung. Respiratory and cardiovascular responses to walking down a traffic-polluted road compared with walking in a traffic-free area in participants aged 60 years and older with chronic lung or heart disease and age-matched healthy controls: a randomised, crossover study. *The Lancet*, Vol. 391, No. 10118, 2018, pp. 339–349.
- 7 Atkinson, R. W., B. Barratt, B. Armstrong, H. R. Anderson, S. D. Beevers, I. S. Mudway, D. Green, R. G. Derwent, P. Wilkinson, and C. Tonne. The impact of the congestion charging scheme on ambient air pollution concentrations in London. *Atmospheric Environment*, Vol. 43, No. 34, 2009, pp. 5493–5500.
- 8 Invernizzi, G., A. Ruprecht, R. Mazza, C. De Marco, G. Močnik, C. Sioutas, and D. Westerdahl. Measurement of black carbon concentration as an indicator of air quality benefits of traffic restriction policies within the ecopass zone in Milan, Italy. *Atmospheric environment*, Vol. 45, No. 21, 2011, pp. 3522–3527.
- 9 Boogaard, H., N. A. Janssen, P. H. Fischer, G. P. Kos, E. P. Weijers, F. R. Cassee, S. C. van der Zee, J. J. de Hartog, K. Meliefste, and M. Wang. Impact of low emission zones and local traffic policies on ambient air pollution concentrations. *Science of the Total Environment*, Vol. 435, 2012, pp. 132–140.
- 10 Karner, A. A., D. S. Eisinger, and D. A. Niemeier. Near-roadway air quality: synthesizing the findings from real-world data. *Environmental Science & Technology*, Vol. 44, No. 14, 2010, pp. 5334–5344.
- 11 Bigazzi, A. Y., and M. A. Figliozzi. Impacts of freeway traffic conditions on in-vehicle exposure to ultrafine particulate matter. *Atmospheric Environment*, Vol. 60, 2012, pp. 495–503.
- 12 Wang, Y., Y. Zhu, R. Salinas, D. Ramirez, S. Karnae, and K. John. Roadside measurements of ultrafine particles at a busy urban intersection. *Journal of the Air & Waste Management Association*, Vol. 58, No. 11, 2008, pp. 1449–1457.
- 13 Kimbrough, S., R. W. Baldauf, G. S. Hagler, R. C. Shores, W. Mitchell, D. A. Whitaker, C. W. Croghan, and D. A. Vallero. Long-term continuous measurement of near-road air pollution in Las Vegas: seasonal variability in traffic emissions impact on local air quality. *Air Quality, Atmosphere & Health*, Vol. 6, No. 1, 2013, pp. 295–305.
- 14 Venkatram, A., V. Isakov, E. Thoma, and R. Baldauf. Analysis of air quality data near roadways using a dispersion model. *Atmospheric Environment*, Vol. 41, No. 40, 2007, pp. 9481–9497.

- 15 Wu, G., P. Hao, L. Pham, H. Jung, and K. Boriboonsomsin. *Prediction of real time particulate matter concentrations on highways using traffic information and emission model*. 2017.
- 16 Choudhary, A., and S. Gokhale. Urban real-world driving traffic emissions during interruption and congestion. *Transportation Research Part D: Transport and Environment*, Vol. 43, 2016, pp. 59–70.
- 17 South Coast AQMD. Near-roadway air monitoring stations. <http://www.aqmd.gov/home/air-quality/air-quality-studies/air-quality-monitoring-studies/near-road-air-network>. Accessed June 30, 2019.
- 18 South Coast AQMD. Annual air quality monitoring network plan—Ontario SR-60. <http://www.aqmd.gov/docs/default-source/clean-air-plans/air-quality-monitoring-network-plan/aaqmp-ontario-route60-nearroad.pdf?sfvrsn=16>. Accessed June 30, 2019.
- 19 South Coast AQMD. Annual air quality monitoring network plan—Long Beach I-710. <http://www.aqmd.gov/docs/default-source/clean-air-plans/air-quality-monitoring-network-plan/aaqmp-longbeach710-nearroad.pdf?sfvrsn=16>. Accessed June 30, 2019.
- 20 U.S. EPA. *Meteorological monitoring guidance for regulatory modeling applications*. Feb 2000. <http://www.epa.gov/scram001/guidance/met/mmgrma.pdf>. Accessed June 30, 2019.
- 21 California Department of Transportation. Performance Measurement System (PeMS). <http://pems.dot.ca.gov/>. Accessed June 30, 2019.
- 22 California Department of Transportation. *PEMS Users Guide*. https://pems.ettp.energy.gov/pems/home/pems_user_guide.pdf. Accessed June 30, 2019.
- 23 Jia, Z., C. Chen, B. Coifman, and P. Varaiya. The PeMS algorithms for accurate, real-time estimates of g-factors and speeds from single-loop detectors. In *Intelligent Transportation Systems, 2001 Proceedings*, pp. 536–541.
- 24 Box, G. E., and D. R. Cox. An analysis of transformations. *Journal of the Royal Statistical Society: Series B (Methodological)*, Vol. 26, No. 2, 1964, pp. 211–243.
- 25 Pearson, K. Note on regression and inheritance in the case of two parents. *Proceedings of the Royal Society of London*, Vol. 58, 1895, pp. 240–242.
- 26 R Development Core Team. R: a language and environment for statistical computing. <http://www.R-project.org>. Accessed June 30, 2019.
- 27 Wu, G., K. Boriboonsomsin, M. Barth, and R. Tadi. Comparative analysis of empirical capacities between freeways with different types of high-occupancy vehicle (HOV) access control. Transportation Research Board Annual Meeting, 2015, Washington, D.C.
- 28 Friedman, J. H. Multivariate adaptive regression splines. In *The Annals of Statistics*, 1991, pp. 1–67.
- 29 Seinfeld, J. H., and S. N. Pandis. *Chapter 6: Atmospheric chemistry and physics: from air pollution to climate change*. John Wiley & Sons, 2016.
- 30 Seagram, A. F., S. G. Brown, S. Huang, K. Landsberg, and D. S. Eisinger. National assessment of near-road air quality in 2016: multi-year pollutant trends and estimation of near-road PM_{2.5} increment. *Transportation Research Record*, Vol. 2673, No. 2, 2019, pp. 161–171.
- 31 California Air Resource Board. Reid vapor pressure requirements. <https://ww3.arb.ca.gov/fuels/gasoline/rvp/rvp.htm>. Accessed June 30, 2019.
- 32 U.S. EPA. Gasoline Reid vapor pressure. <https://www.epa.gov/gasoline-standards/gasoline-reid-vapor-pressure>. Accessed June 30, 2019.
- 33 South Coast Air Quality Management District. *Air Quality Management Plan 2016 Draft Final*.